Journal of Materials Chemistry B

ROYAL SOCIETY OF CHEMISTRY

PAPER

View Article Online
View Journal | View Issue

Cite this: J. Mater. Chem. B, 2022, 10, 2708

Preclinical testing of an anal bulking agent coated with a zwitterionic polymer in a fecal incontinence rat model†

Jung-Woo Choi,‡[a] Joonbum Lee,‡[b] Yuseon Lee,[c] Ji-Hun Seo *[b] and Kwang Dae Hong*[d]

Received 25th October 2021,
Accepted 3rd February 2022

DOI: 10.1039/d1tb02341a

rsc.li/materials-b

Fecal incontinence is a disabling condition in which the passage of fecal material cannot be controlled. Although the condition is not life-threatening, it can seriously reduce the quality of life of a patient by isolating them from others. Though various surgical treatments are available for moderate to severe symptoms, a bulking agent is a minimally invasive technique that has attracted attention because of its safety and simple treatment process. However, the biocompatibility of bulking agent materials remains a central issue, with their durability questioned because immune responses and/or the circulatory system may remove the bulking agent *in vivo*. This study investigated a bulking agent composed of polydimethylsiloxane and hyaluronic acid as a microfiller and carrier gel, respectively. To improve the injectability of the bulking agent, the filler size was tuned using a suspension-based fabrication technique. To evade immune responses, the filler surface was treated with a zwitterionic polymer that simultaneously functionalized and stabilized the material interfaces. The resulting bulking agent exhibited good injectability and biocompatibility *in vitro*, with 58% lower protein adsorption and no cytotoxicity, leading to an improved bulking effect in a preclinical rat model compared with a bulking agent without surface treatment. These results illustrate the promising potential of bulking agents as a therapy for fecal incontinence with reduced foreign body reactions and long-lasting efficacy.

Introduction

Fecal incontinence (FI) is the involuntary loss of bowel content, including gas, liquid stool and mucus, and/or solid feces. The symptoms are generally a source of severe stress for the patient and can lead to social isolation. It has been estimated that FI affects up to 18% of the population,[1] with childbirth trauma and abnormalities in the anal sphincter complex being the most common causes.[2] When conservative treatments such as antidiarrheal agents and biofeedback fail, surgical intervention is required. The injection of a bulking agent around the anal sphincter muscle can augment the anal cushion and generate a passive barrier to the involuntary passage of a stool. A recent systematic review has found that this procedure exhibits good mid-term outcomes and minimal complications,[3] but the optimal injection material has yet to be determined.

Various materials have been tested for use in bulking agents, including collagen, carbon particles, silicone, dextranomer, and hydroxyapatite. However, none of these satisfy all of the characteristics of an ideal implant: biocompatibility, safety, stability at the implantation site, cost-effectiveness, and no migration.[4] The implantation of a biomaterial inevitably induces the host immune response known as the foreign body reaction (FBR), which consists of a series of inflammatory reactions followed by fibrosis.[5] Nonspecific protein adsorption onto the implant surface is considered the first step in the FBR. The interaction between the adsorbed proteins and the adhesion receptors on the inflammatory cells represents a major cellular recognition system for implanted biomaterials. Thus, the surface properties of the biomaterial are an important factor in modulating the FBR in the first 2–4 weeks following the implantation of the biomaterial, even though the FBR at the interface between the tissue and material will continue for the *in vivo* lifetime of the implant.[6]

Zwitterions are superhydrophilic materials with both cationic and anionic groups, and they can interact electrostatically

[a] Department of Pathology, Korea University Ansan Hospital, Gyeonggi-do, Republic of Korea
[b] Department of Materials Science and Engineering, Korea University, Seoul, Republic of Korea. E-mail: seojh79@korea.ac.kr
[c] Biomedical Research Center, Korea University Ansan Hospital, Gyeonggi-do, Republic of Korea
[d] Department of Colorectal Surgery, Korea University Ansan Hospital, Gyeonggi-do, Republic of Korea. E-mail: drhkd@korea.ac.kr

† Electronic supplementary information (ESI) available. See DOI: 10.1039/d1tb02341a

‡ Contributed equally.

with water molecules to form a hydration layer and inhibit nonspecific protein adsorption.[7] Zwitterionic polymers such as 2-methacryloyloxyethyl phosphorylcholine (MPC), sulfobetaine methacrylate (SBMA), and carboxybetaine methacrylate (CBMA) have shown promise in various medical applications due to their anti-biofouling effects.[8–11] Polydimethylsiloxane (PDMS), which is commonly referred to as silicone, has been used in various medical applications due to its versatile, inexpensive, and nontoxic properties.[12–14] Hence, we hypothesized that if zwitterions are coated onto the surface of a PDMS elastomer, the resulting novel bulking agent could exhibit higher biocompatibility and cost-effectiveness.

In this work, we describe the formation of an injectable PDMS bulking agent and a durable zwitterionic coating thereon to reduce protein adsorption and cellular responses and thus mitigate the FBR. To this end, a hydrogel of hyaluronic acid, a major natural mucopolysaccharide in the body's synovial tissues and one of the most biocompatible materials, was used as an injection carrier. Hyaluronic acid and/or its hydrogels are particularly advantageous for injection purposes because of the lubricating and shear thinning properties.[39,40] Using the proposed biomaterial, we investigated its functional and histological performance in an FI rat model (Scheme 1).

Experimental

Materials

MPC was purchased from KCI, while *n*-butyl methacrylate (BMA) and 1,4-butanediol diglycidyl ether (BDDE) were purchased from Tokyo Chemical Industry. Anhydrous ethanol, diethyl ether, and sodium hydroxide solution (1 M) were purchased from Samchun Chemical. 2,2′-Azobisisobutyronitrile (AIBN) solution (0.2 M in toluene), polyvinylpyrrolidone (PVP), fluorescein isothiocyanate-labeled bovine serum albumin (FITC-BSA), and sodium nitrate was purchased from Sigma-Aldrich. PDMS (Sylgard 184 silicone elastomer) was purchased from Dow. Hyaluronic acid (HA) sodium salt (91%, molecular weight ≥ 1 MDa, from *Streptococcus equi*) was purchased from Alfa Aesar. Deionized water was prepared using an ultrapure water system (Milli-Q IQ 7000) from Merck Millipore. A regenerated cellulose dialysis membrane (SpectraPor; molecular weight cut-off, 12–14 kDa) was purchased from Repligen. For the cell cultures, an embryotic mouse fibroblast cell line (NIH/3T3) was taken from the Korean Collection for Type Cultures (KCTC). Phosphate-buffered saline (PBS) was purchased from Welgene and other bioreagents, including Dulbecco's phosphate-buffered saline, trypsin-EDTA solution (0.25%), Dulbecco's modified Eagle's medium (DMEM), and newborn calf serum (NBCS), were purchased from Gibco. A water-soluble tetrazolium salt solution (Cell Counting Kit-8) was purchased from Dojindo for cell viability and proliferation assays. The ^{1}H nuclear magnetic resonance (NMR) spectrum of the synthesized copolymer was obtained using a Mercury NMR spectrometer system (400 MHz) from Varian. The molecular weight of the polymer was analyzed using a YL9100 gel permeation chromatography (GPC) system from YL Instruments equipped with an analytic column with aqueous stationary phases (Ultrahydrogel 1000) from Waters, using poly(ethylene oxide) standards and an aqueous sodium nitrate solution (0.2 M) as the mobile phase. The elemental composition of the polymer surface was assessed using an X-ray photoelectron spectrometer system (K-Alpha^{+}) from Thermo Scientific. A plate photometer (Multiskan FC) from Thermo Scientific was used for colorimetric assays. An inverted microscope (Eclipse Ts2-FL) equipped with a color camera (DS-Fi3) and imaging software (NIS-Elements) from Nikon were utilized to collect and analyze microscopic images and the routine culture of cells. A motorized force tester (MultiTest-dV) from Mecmesin was used to measure compression forces.

Preparation of the injectable bulking agents

Synthesis of the zwitterionic copolymer. The monomers, MPC (738.2 mg, 2.5 mmol) and BMA (355.5 mg, 2.5 mmol),

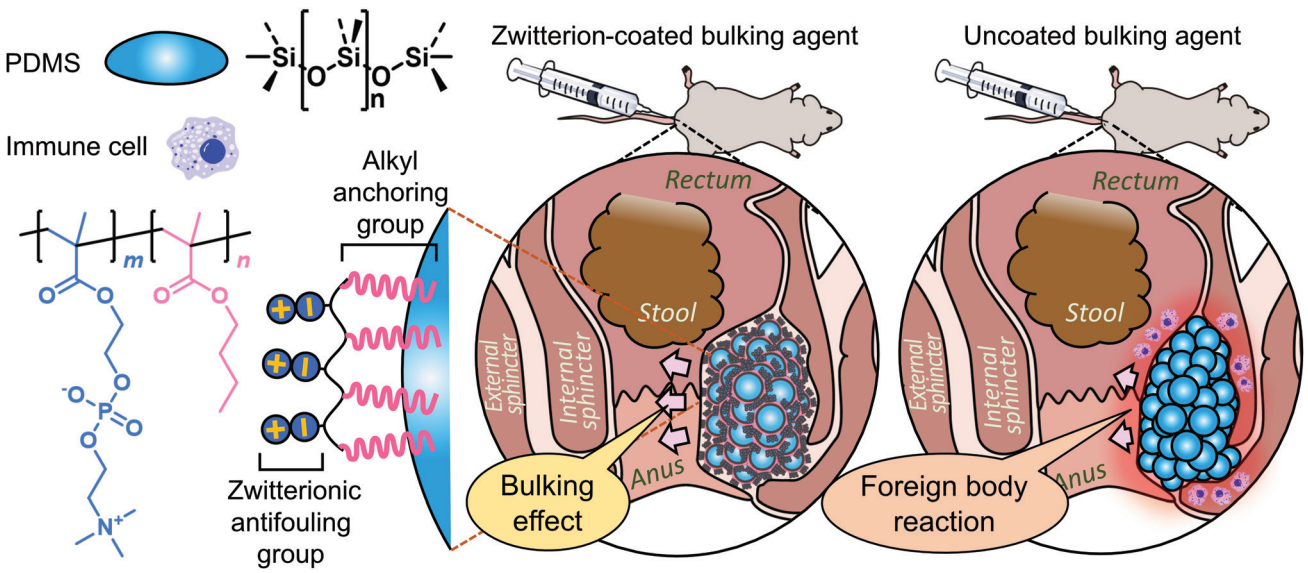

Scheme 1 Schematic representation of the fabrication of zwitterion-coated bulking agent and its preclinical testing. PDMS, polydimethylsiloxane.

were added to anhydrous ethanol (5 mL) in a glass vial. After the mixture had become clear, the vial was sealed using a rubber septum, and the mixture was subjected to argon sparging for 10 min to remove dissolved gasses. After 125 μL of AIBN (25 μmol) solution was added to the mixture using a syringe, the mixture was heated at 60 °C for 12 h for polymerization. After cooling to 25 °C, the polymer was reprecipitated by the dropwise addition of the mixture to excess diethyl ether (300 mL). The precipitants were filtrated and dried under a vacuum to obtain the purified zwitterionic copolymer poly[(2-methacryloyloxyethyl phosphorylcholine)-*co*-(*n*-butyl methacrylate)] (PMB) as a white powder.

Preparation of PDMS fillers. An aqueous PVP solution (7.5 wt%) and PDMS (10:1 mixing ratio of base to curing agent) were added to a 70 mL cylindrical vial. The mass fraction of PDMS to the PVP solution was 15 wt% or 25 wt% within a total mass of 24 g. After 1 h of magnetic stirring at 25 °C, the vial was transferred to an oil bath at 60 °C and cured for 1 h. PMB (20.4 mg) was added to the vial to produce zwitterion-coated PDMS particles, and the mixture was further cured at 60 °C for 5 h. During the process, 2 different stirring speeds (650 and 1100 rpm) were adopted. After cooling to 25 °C, the mixture was moved to a centrifuge tube and subsequently centrifuged and decanted several times to reduce the content of PVP and water-suspended small particles. The water was finally freeze-dried to obtain refined PDMS particles.

Preparation of bulking agents with hyaluronic acid carrier gels. HA sodium salt (100 mg) was added to deionized water (750 μL) in a glass vial. Sodium hydroxide solution (250 μL) and BDDE (15 μL) were added to the vial and mixed thoroughly. The solution was then heated at 50 °C for 3 h to crosslink the HA. The resulting solidified gel was transferred to a dialysis membrane and immersed in PBS solution (1.5 L) for 7 days to attain physiological pH and osmolarity. The resulting HA gels and PDMS particles were then mixed to produce the final products, whose ratio of PDMS to the HA gel was 4:6 by weight. All of the injectable bulking agents (*i.e.*, zwitterion-coated PDMS/HA [ZcPH], uncoated PDMS/HA [UcPH], and HA) were transferred to hypodermic syringes (BD, cat. 309628) before use. The injectabilities of the particle solutions were measured in compression testing, at a speed of 3 mm min^{-1}, until the displacement of a syringe plunger reached 10 mm.

In vitro biocompatibility of the injectable bulking agents

Protein adsorption on the material surface. FITC-BSA (4.5 mg) was dissolved in PBS (1 mL) at 37 °C for 0.5 h using a glass vial. PDMS particles (ZcPH or UcPH; 100 mg) were then added to the vial, which was placed in a water bath at 37 °C for 2 h. During warming, the vial was gently agitated every 0.5 h to refresh the contact between the particle surface and the FITC-BSA solution. After protein adsorption, the PDMS particles were washed 3 times using PBS (3 × 5 mL). The particles were then transferred to a 24-well cell culture plate for observation under an optical microscope. To quantify the protein adsorption levels, epifluorescent and diascopic micrographs were taken, and regions of interest were set in the epifluorescent images by referring to the particle boundaries in the diascopic images. The protein adsorption levels were presented as the mean fluorescence intensity recorded by imaging software.

Cytotoxicity of the injectable bulking agent. The cytotoxicity of ZcPH, UcPH, and HA was evaluated using a modified form of ISO 10993-5. Murine fibroblasts were subcultured several times in an incubator (37 °C, 5% CO_2) before the test. DMEM supplemented with 9% NBCS was used as a complete culture medium. The cells were seeded in 48-well plates (4×10^4 cells per well) and incubated for 22 h. After a subconfluent cell layer was confirmed under an optical microscope, the culture medium was aspirated. The injectable bulking materials were then placed in the centers of the wells. As a direct contact cytotoxicity test, 4 μL droplets of each bulking agent were used to cover approximately 1/10 of the area of the cultured cells in the wells (0.75 cm^2). After fresh culture medium (0.8 mL) was gently added without disturbing the materials, the cells were incubated for a further 24 h or 48 h. After morphological changes to the cells were observed, the culture medium was removed and a fresh culture medium with a 10% water-soluble tetrazolium salt solution was added. After incubation for 2 h, the optical density at 450 nm was measured using a plate reader.

In vivo biocompatibility tests of the injectable bulking agent

Animal study design. Eighteen 10-week-old Sprague-Dawley female rats were employed as the experimental animal. After a week of monitoring, the rats were divided randomly into 3 groups, with 6 rats in each group. The weight deviation among groups was from 140 to 180 g. The animals were anesthetized using inhaled isoflurane. They were intramuscularly injected with 5 mg kg^{-1} of ketoprofen as a painkiller and 5 mg kg^{-1} of enrofloxacin as an antibiotic. A 5 mm Bovie incision was made on the posterior side of the anus. The injection procedure was performed 1 week after the sphincter injury. Six of the rats were injected with ZcPH, 6 with UcPH, and 6 with HA solution, respectively. All animals had 0.1 cc of each material injected into the posterior side of the anus at a depth of 6–8 mm parallel to the rectum using a 1 mL syringe and an 18G needle (Fig. 1a). Three rats from the same group were placed in a cage. Rats were examined by the researcher (L. S.) twice a week. Any sign of local or systemic infection was observed and recorded.

Three animals per group were sacrificed at intervals of 1 week and 4 weeks after the injection treatment. The rats were anesthetized using inhaled isoflurane and killed with concentrated CO_2 gas in the designated euthanasia chamber. The anus, perianal region, and rectum were removed together to protect the condition of the injected materials (Fig. 1b and c)

The lungs, liver, kidney, and iliac lymph node were also excised. A manometric evaluation was only performed on the 9 rats that were sacrificed 4 weeks after injection treatment. Manometry was taken at baseline, after the sphincter injury, and 1 week and 4 weeks after injection treatment.

All experimental procedures were approved by the Animal Ethics Committee of Korea University College of Medicine (IRB No. KOREA-2019-0037).

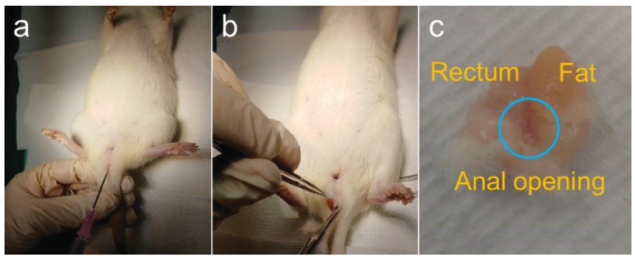

Fig. 1 Bulking materials implanted around the anus removed along with surrounding tissues. (a) At the beginning, 0.1 cc of each bulking material was injected into the posterior side of the anus. (b) Perianal tissue was excised en bloc to avoid hindering the locoregional relationships. (c) The bulking material (blue circle) was surrounded by thin connective tissue and adhered to the distal perirectal space.

Anal manometric evaluation. All examinations were conducted under inhaled isoflurane anesthesia without any muscle relaxation. We used a saline-filled latex balloon (size 4, ADInstruments, Germany) connected through PE50 tubing to a pressure transducer (BP100, iWorks Systems, Dover, USA) and a physiological data acquisition system (IX-RA-834 with LabScribe Software, iWorks Systems, Dover, USA) for anal manometric measurement. After the balloon was inflated to a pressure of 10–12 mmHg, calibration of the system was conducted. The balloon probe was inserted into the anal canal up to 6–8 mm above the opening of the anus. After a 5 min adaptation period, spontaneous contraction waves were recorded for 5–10 min. To determine the resting pressure, the balloon probe was drawn out in a contraction interval, and the resulting difference from the baseline pressure (the mean of 5 intervals) was calculated[15] (Fig. 2).

Tissue preparation and microscopic evaluation. The harvested tissue was fixed in 10% formalin. The rectum was divided transaxially including the mid-portion of injected materials. Two remote cutting was performed for distant organs. Each tissue section was embedded in paraffin, and they were fabricated at a thickness of 4 μm, followed by hematoxylin and eosin (H&E) staining for observation with a light microscope. The size of the implant was measured using the length of the longest axis on the slide.

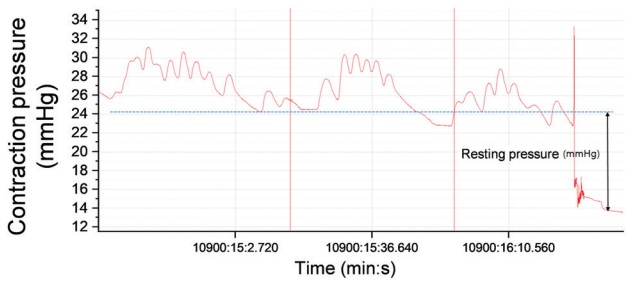

Fig. 2 Anal manometry demonstrating spontaneous contraction waves. The balloon probe was drawn out in a contraction interval and the resulting difference from the baseline pressure was taken to be the resting pressure.

Microscopic evaluation of the local immune reaction at the perianal injection site and the systemic migration of the implant to the distal organs was conducted blind by one pathologist (J.-W. Choi). When evaluating the local immune response, the number of cells per high-power field (×400) around the implant was counted and assigned FBR, inflammatory, and fibrosis scores. Each score was measured as the average of 3 different areas, which was estimated to be the highest score in the low-power field (×100).

The FBR score reflects the immune response sequence based on the severity of the inflammatory reaction and the extent of tissue repair.[16] The inflammatory score measures the acute inflammatory response and is divided into 5 stages from 0 to 4 depending on the severity of the inflammation. The inflammatory cells counted are polymorphonuclear cells, lymphocytes, eosinophils, and plasma cells. The fibrosis score indicates the severity of fibrosis in the tissue repair process and is also divided into 5 stages from 0 to 4 depending on the thickness of the fibrotic band. (Table 1). The systemic migration of injected materials was assessed by identifying whether there were any foreign materials or an inflammatory reaction in distant organs.

Statistical analysis. Repeated-measures ANOVA was used to compare the sequential manometric values for 9 rats (3 per group) that were followed for up to 4 weeks after the injection treatment. For microscopic evaluation, Friedman tests were performed to compare the differences for 18 rats (6 per group) 1 and 4 weeks after the injection treatment. Turkey's tests were used for *post hoc* comparisons. The data were summarized as the mean and standard error. Values of $p < 0.05$ were considered to be statistically significant. Data analyses were performed using SPSS 20.0 (IBM SPSS Statistics, NY, USA).

Results

Preparation of the injectable bulking agents

Copolymerization of the zwitterionic polymer. The molecular composition of the synthesized zwitterionic copolymer was determined using ^{1}H NMR spectroscopy, showing that the molar zwitterionic monomer composition was 0.48, similar to the molar feed ratio of 0.50 (ESI† Fig. S1). GPC revealed that the weight-average molecular weight of the zwitterionic copolymer was 2.8×10^4 and the molecular-weight dispersity ($Đ_M$) was 3.93 (ESI† Fig. S2).

Size tunability of the bulking agent. The diameters of the PDMS particles produced according to the PDMS ratio and the stirring speed led to the formation of 2 distinctive groups. The particles prepared at 650 rpm had diameters of 118.4 ± 28.3 μm (mean ± SD) and 118.4 ± 33.0 μm for PMDS ratios of 25 wt% and 15 wt%, respectively. The particles prepared at 1100 rpm had diameters of 80.3 ± 16.5 μm and 88.3 ± 17.8 μm for PMDS ratios of 25 wt% and 15 wt%, respectively (Fig. 3). There was no significant difference in the particle diameters for different PDMS ratios ($q = 2.685$, $p = 0.058$), while the effect of the stirring

Table 1 Microscopic semi-quantitative evaluations for implant sites

	Score			
Category	0 1	2	3	4
Inflammatory score[a]	0 Rare, 1–10/HPF	10–30/HPF	Heavy infiltrate	Packed
Fibrosis score	0 Narrow band	Moderately thick band	Thick band	Extensive band
FBR score[b]	0 Slight reaction with a few inflammatory cells	Clear inflammatory reaction with 1 or 2 giant cells	Fibrous tissue with inflammatory cells and giant cells	Granuloma with encapsulated implants—clear FBR

[a] Polymorphonuclear cells, lymphocytes, eosinophils, and plasma cells are counted. [b] The FBR score, established by Duranti *et al.*, represents the immune response sequence based on the severity of the inflammatory reaction and the extent of tissue repair.[16] HPF, high power field (× 400); FBR, foreign body reaction.

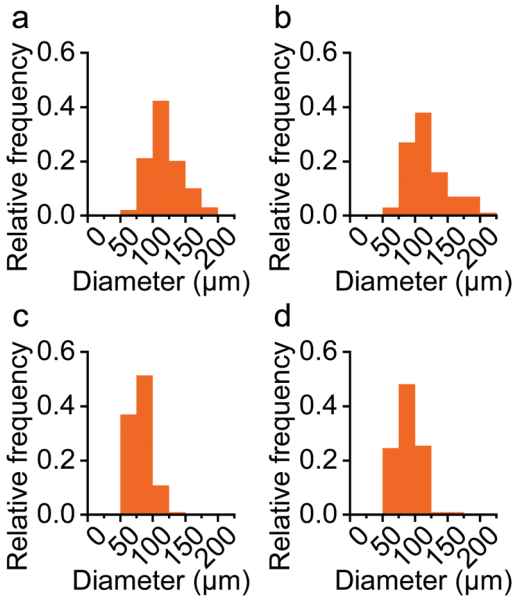

Fig. 3 Size distributions of the PDMS particles for bulking agents (n = 100 for each distribution). The effects of the PDMS ratio and stirring speed on the particle diameter were investigated. The size histograms of the particles fabricated using (a) 25 wt% PDMS ratio and the stirring speed of 650 rpm; (b) 15 wt% PDMS ratio and the stirring speed of 650 rpm; (c) 25 wt% PDMS ratio and the stirring speed of 1100 rpm; and (d) 15 wt% PDMS ratio and the stirring speed of 1100 rpm.

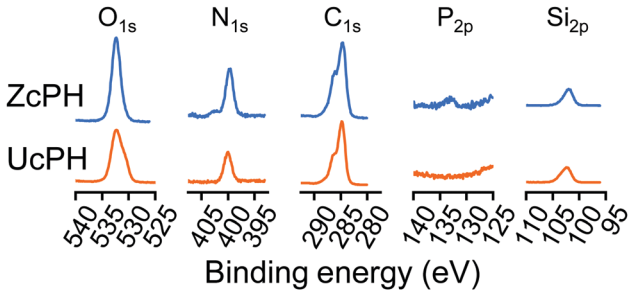

Fig. 4 Elemental composition of the zwitterion-coated particle surface assessed using XPS. Narrow scan spectra within the O_{1s}, N_{1s}, C_{1s}, P_{2p}, and Si_{2p} regions. ZcPH, zwitterion-coated polydimethylsiloxane hyaluronic acid solution; UcPH, uncoated polydimethylsiloxane hyaluronic acid solution.

speed was statistically significant (q = 20.206, $p < 0.001$; two-way ANOVA, α = 0.05).

Surface characterization of the zwitterion-coated bulking agent. The zwitterionic polymer was incorporated with the particles prepared using a PDMS ratio of 25 wt% and a stirring speed of 650 rpm. The elemental composition of the zwitterion-coated particle surface (ZcPH) was determined using XPS and compared to the control (UcPH). Common major peaks were observed in the O_{1s}, N_{1s}, C_{1s}, and Si_{2p} regions in the survey scan spectra (ESI† Fig. S3). In the narrow scan spectra, slight peaks at 402 eV (a shoulder peak) and 133 eV were only observed for ZcPH (Fig. 4).

In vitro biocompatibility of the injectable bulking agent

Protein adsorption on the material surface. After protein adsorption, the ZcPH particles had a significantly lower fluorescent intensity of 6.01 ± 0.50 (mean ± SD) compared to the fluorescent intensity of the UcPH particles, which was 14.48 ± 1.17 (q = 18.844, $p < 0.001$; Tukey's test, α = 0.001) (Fig. 5).

Cytotoxicity of the injectable bulking agent. In the cytotoxicity testing based on direct contact, both the changes in cellular morphology and cell proliferation after exposure to the foreign materials were investigated. After 24 h and 48 h of contact with the bulking agents, none of the cells exhibited a noticeable change in their morphology (ESI† Fig. S4). The quantitative determination of cell viability and proliferation using colorimetric assays also showed that the relative cell numbers in all cultures were not significantly different compared to the controls which were cultured without any potential cytotoxic agents (Fig. 6).

Animal tests

The rats did not exhibit any abnormal behavior or signs of infection during the experimental period. The perianal lesions also appeared generally normal.

Anal manometric evaluation. The resting pressure after surgery was lower compared to the baseline in all 3 groups, with no significant difference between the groups (ZcPH, 12.74 ± 3.36 mmHg; UcPH, 11.67 ± 2.28 mmHg; HA, 12.72 ± 0.18 mmHg; p = 0.788). Four weeks after the injection treatment, the resting pressure in the ZcPH group was higher than in the UcPH and HA groups, though this was not significant

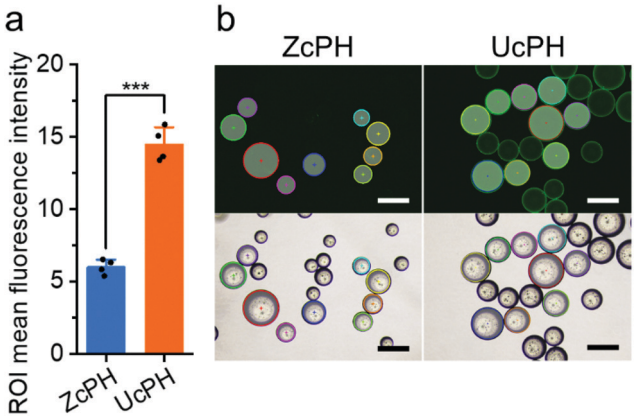

Fig. 5 Protein adsorption tests on the ZcPH and UcPH particles. (a) Comparison of the mean fluorescence intensity of the adsorbed FITC-BSA (mean ± SD; Tukey's test; ***$p < 0.001$). (b) Optical and fluorescent microscopic images of ZcPH and UcPH after protein adsorption. The circular borders with central dots indicate the regions of interest (ROI) used to determine the mean fluorescence intensity. Bar, 250 μm. ZcPH, zwitterion-coated polydimethylsiloxane hyaluronic acid solution; UcPH, uncoated polydimethylsiloxane hyaluronic acid solution.

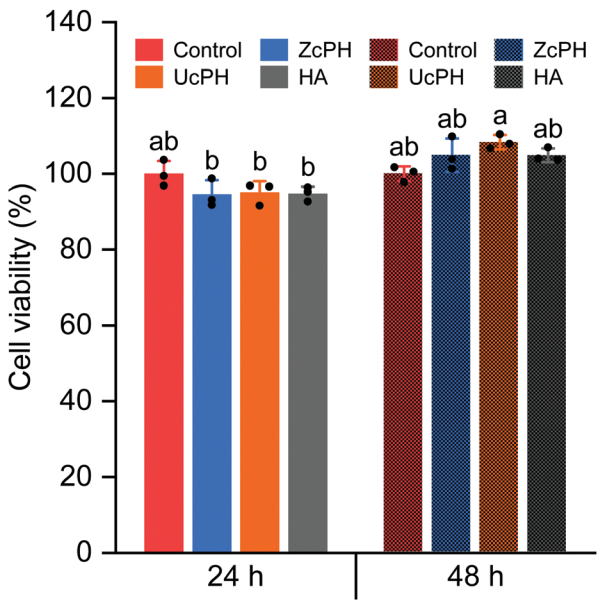

Fig. 6 Cytotoxicity of the injectable bulking materials 24 and 48 h after direct contact. A cell culture without any foreign material was set as the control and the cell numbers relative to the control are presented as the percent cell viability (mean ± SD). The alphabetical letters group statistically equal means and therefore the means that do not share a letter are statistically different (one-way ANOVA, $\alpha = 0.001$; Tukey's multiple comparisons test, $\alpha = 0.001$). ZcPH, zwitterion-coated polydimethylsiloxane hyaluronic acid solution; UcPH, uncoated polydimethylsiloxane hyaluronic acid solution; HA, hyaluronic acid solution.

(ZcPH, 19.48 ± 7.81 mmHg; UcPH, 14.63 ± 3.51 mmHg; HA, 12.74 ± 2.78 mmHg; $p = 0.330$). Overall, this analysis revealed that the anal resting pressure did not differ according to the

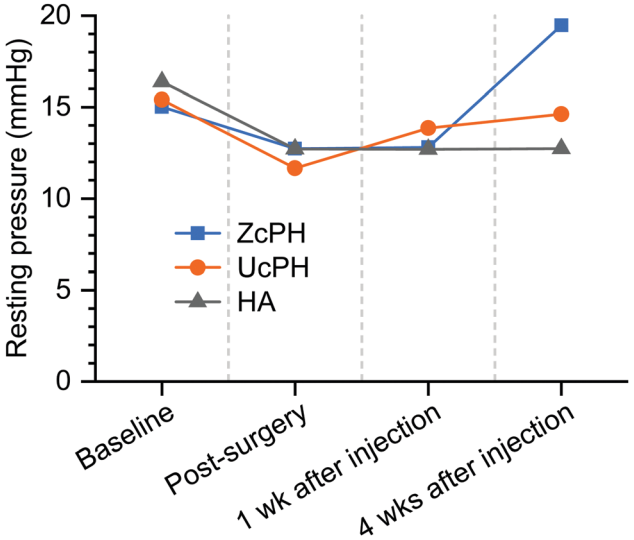

Fig. 7 Sequential changes in the anal resting pressure according to injected bulking materials. Two-way repeated-measures ANOVA indicated that there were no statistical differences in the resting pressure between the groups at each time point (Mauchly's $W = 0.517$; $df = 5$; $p = 0.687$). ZcPH, zwitterion-coated polydimethylsiloxane hyaluronic acid solution; UcPH, uncoated polydimethylsiloxane hyaluronic acid solution; HA, hyaluronic acid solution.

injected material over the 4-week observation period (Mauchly's $W = 0.517$; $df = 5$; $p = 0.687$) (Fig. 7).

Descriptive analysis of the local immune reaction. Both ZcPH and UcPH formed well-demarcated space-occupying lesions consisting of variably sized refractile spheres with the infiltration of various inflammatory cells such as lymphocytes, histiocytes, and multinucleated giant cells. In contrast, HA exhibited a local dissection and permeation between the tissues at the injection site with few multinucleated giant cells. After 1 week, the tissues with ZcPH and UcPH had fewer inflammatory cells than those with HA; however, the inflammatory reaction became stronger over time for all of the injected materials (Fig. 8).

Histologic scoring of the local immune reaction. The size of ZcPH was better preserved over time than that of other materials, but this difference was not statistically significant (group: $F = 2.061$, $p = 0.170$; time: $F = 2.217$, $p = 0.162$). The FBR and fibrosis scores were higher 4 weeks after injection than after 1 week ($F = 12.000$, $p = 0.005$ [FBR score]; $F = 10.125$, $p < 0.008$ [fibrosis score]). The FBR score differed between the groups ($F = 21.000$, $p < 0.001$), with the *post hoc* analysis revealing a significant difference between ZcPH and HA (mean difference, 1.50; $p < 0.001$) and between UcPH and HA (mean difference, 1.00; $p = 0.003$), but not between ZcPH and UcPH (mean difference, 0.50; $p = 0.127$). ZcPH has the lowest inflammatory score at all time points (group: $F = 5.571$, $p = 0.019$; time: $F = 0.571$, $p = 0.464$). In *post hoc* analysis, while ZcPH was significantly different from HA (mean difference, 1.17; $p = 0.018$), the difference between ZcPH and UcPH was only marginally significant (mean difference, 0.83; $p = 0.092$). UcPH and HA had no difference (mean difference, 0.33; $p = 0.635$). ZcPH

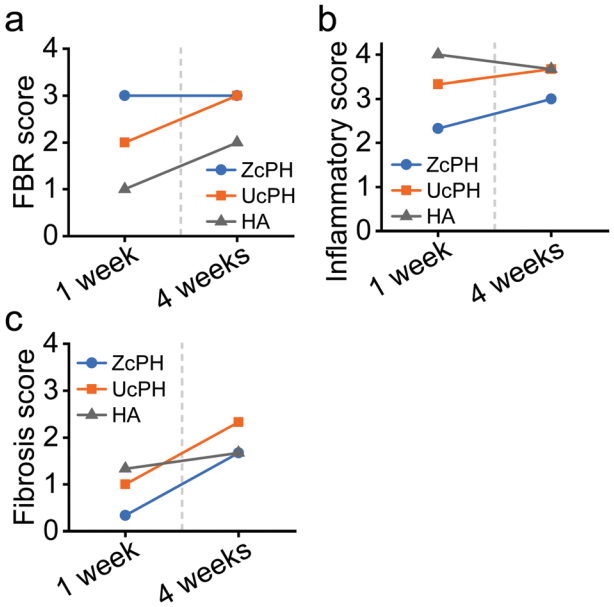

Fig. 8 Semi-quantitative histological scoring for the local immune reactions. (a) FBR score, established by Duranti *et al.*, illustrating the inflammatory reaction and tissue repair. (b) Inflammatory score measuring the acute inflammatory response to the implants. (c) Fibrosis score, which indicates the severity of fibrosis in the tissue repair process. FBR, foreign body reaction; ZcPH, zwitterion-coated polydimethylsiloxane hyaluronic acid solution; UcPH, uncoated polydimethylsiloxane hyaluronic acid solution; HA, hyaluronic acid solution.

had a lower fibrosis score compared to UcPH, but there was no statistical difference between the groups ($F = 1.625$, $p = 0.237$). The fibrosis score also increased over time ($F = 10.125$, $p = 0.008$) (Fig. 9).

Systemic migration. When examining the serial tissue sections from distant organs including the lungs, liver, kidney, and iliac lymph node, the injected materials and their decomposition products were not detected histologically. In addition, there was no abnormal inflammatory reaction such as an allergic or foreign body response due to the possible migration of the injected materials.

Discussion

Size tunability of the injectable bulking agent. Controlling the size of the filler particles in injectable bulking agents is crucial for 3 reasons. First, the size needs to be large enough to avoid local immune reactions and systemic migration. Particles smaller than 20 μm can be phagocytosed by macrophages and the particle migration to distant organs in the blood or lymphatic vessels, leading to granuloma formation, can be prevented when 99 vol% of particles exceed 80 μm.[17,18] Second, particles need to be small enough to preserve injectability. Large particles require wide-diameter needles, which can increase the pain for patients. The resulting increase in the injection force also makes it difficult for surgeons to perform the procedure correctly.[19] Third, the optimal particle size varies depending on the application. For example, Renú, an injection material for vocal cord augmentation, has a particle size that is 2–3 times smaller than Restylane, a dermal filler for facial tissue.[20] Restylane itself has several product lines with different filler sizes depending on the cosmetic purpose and injection depth/site.[21] Overall, particles with a diameter of several tens to hundreds of microns are suitable for injectable bulking agents. Of the several polymerization methods available, such as emulsion, suspension, precipitation, and dispersion polymerization, this study adopted suspension polymerization because it can produce a similar size range.[22] Using suspension polymerization, the size of the polymer particles can be empirically determined by the following equation:[23]

$$\bar{d} = k\frac{D_v \cdot R \cdot \upsilon_d \cdot \varepsilon}{D_s \cdot N \cdot \upsilon_m \cdot C_s} \quad (1)$$

where $\bar{d}$ is the average particle diameter, k is the apparatus design factors, D_v is the diameter of the vessel, D_s is the diameter of the stirrer, R is the volume ratio of the dispersed phase to the suspension medium, N is the stirring speed, υ_d is the viscosity of the dispersed phase, υ_m is the viscosity of the suspension medium, ε is the interfacial tension between the 2 immiscible phases, and C_s is the stabilizer concentration.

The present study attempted to control the size of the particles by varying the volume ratio of the 2 phases (R) and the stirring speed (N) because these factors are easily controllable.[23] The reduction in the particle diameter at a higher stirring speed was reflective of Equation 1. The distribution was also narrower for the smaller particles, which is in line with a previous report.[24] However, R did not significantly affect the particle diameter. Because the volume ratio may have a limited effect on the particle sizes in a given system,[25] it appears that the volume ratio in this study exceeded the critical ratio for size tunability. The volume fractions of PDMS employed in this study were favorable for high productivity,[25] given that bulking agents in which PDMS particles account for 40% of the total weight were required. Overall, the results demonstrated that the particle size was adjustable to some extent by simply altering a single variable. For the *in vivo* injection purposes, the results confirmed that the mean particle size exceeded 118 μm to avoid phagocytosis and systemic migration. After being mixed with HA gel carriers, the injectability was investigated. The particles were not injectable without HA carriers while suitable injectability of the injection force under 0.9 N through a syringe with an 18G needle was confirmed with HA gel carriers (ESI† Fig. S5). With further optimization employing sophisticated reactor designs, strong quality control, such as high uniformity, could be achieved. Thus, it is expected that the size tunability of this method offers a wider range of potential applications that are in compliance with the requirements of injectable bulking agents.

Protein adsorption test. Protein adsorption has been an important factor in determining the biocompatibility of materials. Recognized by cell-binding motifs in cells or bacteria, adsorbed proteins can either cause immune responses that result in severe fibrosis or generate a biofilm on the biomaterial surfaces for microorganisms, leading to infectious complications. The significantly lower protein adsorption demonstrated

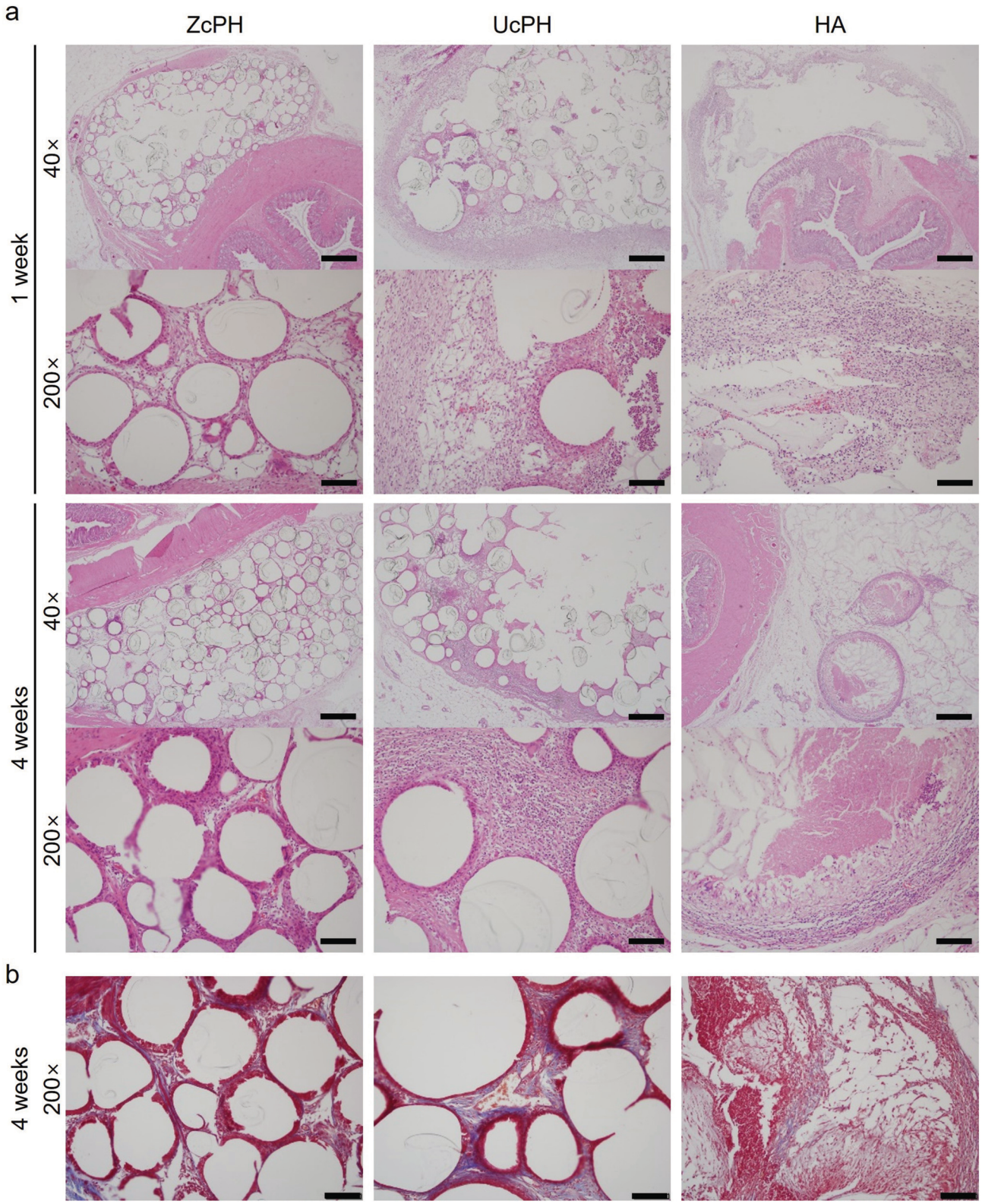

Fig. 9 Histological images of perianal tissues injected with bulking materials at various time points. (a) H&E staining images 1 and 4 weeks after injection treatment. (b) MT staining images 4 weeks after injection treatment. Scale bar, 500 μm (×40) or 100 μm (×200). ZcPH, zwitterion-coated PDMS HA solution; UcPH, uncoated PDMS HA solution; HA, hyaluronic acid solution.

by ZcPH particles compared to UcPH particles indicated that the zwitterionic-coated surface prevented protein adsorption. This can be attributed to the fact that the zwitterion-functionalized superhydrophilic surface forms a hydration

layer, preventing the deposition of proteins. Previous studies have confirmed the effectiveness of zwitterion-coated surfaces in preventing protein adsorption to various biomedical devices, including catheters and ophthalmic lenses.[38]

Materials that have been subject to zwitterionic treatment include PET, PC-based urethanes, Ti alloys, PTFE, and PDMS.[26–29] Of these materials, PDMS has received significant attention because of its softness as an elastomer, which facilitates mechanical adaptation to the surrounding tissue.[30] However, it is well-known that the hydrophobic recovery of the PDMS surface limits long-term functionality.[31] This interfacial phenomenon results from polymer chain rearrangements that minimize the difference in surface energy at the contact between the hydrophobic air and transiently functionalized PDMS surface.[32] In the present study, the zwitterion-coated PDMS particles were encapsulated in HA carrier gels. In this way, it is believed that the functionalization of the PDMS surface was maintained for a period of time until the protein adsorption tests were conducted. The independent trials in the protein adsorption tests included data collected 1 month after the preparation of the materials. This could also be a proxy for assessing the stability of the modified surfaces and provided a rationale for the following *in vivo* biocompatibility tests in a rat model.

Cytotoxicity assay. Testing cytotoxicity is imperative in evaluating the biocompatibility of medical devices prior to *in vivo* use.[33] Because HA constitutes a major component of animal skin, it was assumed that the injectable bulking agent used in the present study would be highly biocompatible. Indeed, there was no indication of cytotoxicity for either ZcPH or UcPH. Although it has been reported that crosslinking agents for HA, such as poly(ethylene glycol) diglycidyl ether and divinyl sulfone, can exhibit damaging effects, BDDE, the crosslinker used in this study, is known to be the safest and most widely used chemical reagent for commercials.[34,35] The byproducts and residuals of BDDE-related species include slight traces of hydrolyzable substances in the human body.[35] Moreover, the fabrication process already included dialysis steps that removed unwanted molecules. The low toxicity of the bulking agents was highlighted by the lack of any abnormal change in the cellular morphology after direct contact testing. Large volumes of the bulking agents could not be tested because the saline in the bulking agents may significantly dilute the essential nutrients in the culture medium. Covering large areas of the cell monolayers may also hinder material exchange. Nonetheless, *in vitro* biocompatibility was confirmed using this method before *in vivo* injections of the bulking agents.

***In vivo* animal testing.** A space-occupying material injected into the perianal sphincter muscle could theoretically push the rectal mucosa intraluminally and lead to an increase in anal resting pressure. This means that bulking materials can act as a passive barrier as an axis of FI treatment.[14] We investigated changes in the resting pressure *via* anal manometry to compare the effectiveness of the bulking materials. The resting pressure in the ZcPH group was higher than that in the UcPH and HA groups during the final follow-up, but this difference was not significant. This lack of significant difference could be because, even in clinical practice, the resting pressure following an injection exhibits mixed results.[3] Because the mechanisms underlying the function of bulking agents have not yet been clearly explained, the physiological responses have been variable. In particular, in human studies, the results can be interpreted using various indicators, such as rectal sensation and maximal tolerable volume, that can be measured *via* communication with the patient in addition to anal resting pressure using anal manometry. In addition, the follow-up period in the present study may have been too short to detect differences in the durability of the materials. It can be seen in the same context that differences in the size of the injected substances did not produce any statistical differences. Because only HA fillers without core particles have been reported to last 3–12 months in tissue, a longer observation period is necessary.[16] Another possible explanation is that, although a few studies using FI rat models have been conducted and the feasibility of the process has been proven, larger animal models may be more suitable when investigating the exclusive action of the anal sphincter.[36] The anal sphincter complex in rats is only a few millimeters thick, which could affect the accuracy of the pressure measurements of the anal canal and the precision of the 5 mm Bovie incision in the sphincter muscle.

In accordance with other reports, the FBR in the local tissue in our rat model was mild, with multinucleated giant cells, macrophages, fibroblasts, and collagen deposits.[18] This FBR did not cause tissue destruction, thus implants using PDMS and/or HA materials appear to have potential for use in medical applications. Semi-quantitative histological scores were used to compare the local immunological response between the materials. The FBR score for the ZcPH and UcPH groups was similar during the final follow-up but, when the immune response was separated into the early inflammatory reaction and the late fibrotic reaction, the ZcPH group exhibited a weaker reaction at both points of the observed period compared to the UcPH group.

The inflammatory score reflects the early FBR, which usually reaches a peak 1–4 weeks after implantation.[6] Our experimental period was thus sufficient to investigate this indicator. During this period, the ZcPH group had a lower inflammatory score than the HA group, although this was not statistically significant. This may suggest that zwitterionic-coated surfaces prevent protein adsorption and consequently reduce the inflammatory reaction.

The fibrosis score reflects the late FBR. Although the exact mechanisms underlying the FBR remain unclear, fibrotic activity can be affected by chronic inflammatory stimuli driven by the macrophages and fibroblasts surrounding the implants. This differs from normal tissue healing and can be as persistent as the tissue repair process.[6,37] The formation of a thick fibrotic capsule around implants is considered a critical step as a means to avoid phagocytosis, increase the volume of the implant, and prevent local migration within the tissue plane.[12,14] However, Harlim *et al.* recently classified the FBR of silicone implants into mild or severe forms depending on the

degree of fibrosis and suggested that, when an inflammatory response was followed by mild fibrosis, implants would be more preserved and the surrounding tissue would be less damaged.[37] We also believe that the excessive formation of fibrotic capsules between implants and tissue can disturb the integration of the implant and reduce its long-term function.

It is possible that the experimental period was too short to fully investigate the fibrotic process associated with the implants. Given that the ZcPH group had a lower fibrosis score than the UcPH group at both follow-up points, continuous experiments could be performed to evaluate the possibility that zwitterionic-coated PDMS can help to attenuate chronic inflammation and reduce fibrotic activity. In particular, further studies investigating changes in the inflammatory mediators and the extracellular matrix around the implants are crucial. No signs of foreign materials or inflammation were observed in the resected distant organs. Most PDMS particles in the filler exceeded 100 μm in diameter, hence systematic migration was expected to be inherently unlikely. However, this also needs to be confirmed *via* repeated experiments at different injection sites.

Conclusions

In conclusion, a newly proposed tissue bulking agent was tested for the treatment of FI in a preclinical rat model. A zwitterionic polymer was employed for the surface treatment of PDMS, and the fabrication process was controlled to improve the biocompatibility, injectability, and size tunability of the resulting bulking agent. Although statistical differences were not derived from *in vivo* experiments, the ZcPH showed a tendency to maintain a higher anal resting pressure 4 weeks after treatment and produced better histological scores for the local immune reaction compared to the UcPH bulking agent. In spite of the fact that investigations using larger animal models with longer follow-up periods are required to confirm these findings, the results indicate that the low durability of bulking agent therapy, which has been identified as an inherent drawback of this therapy, can be improved with the suitable selection and tuning of the bulking materials.

Conflicts of interest

There are no conflicts to declare.

Acknowledgements

This study was supported by a grant from Korea University College of Medicine and Korea University Ansan Hospital. This research was also supported by ATC+ Program (20014029) funded by Korea Evaluation Institute of Industrial Technology.

References

1 A. K. Macmillan, A. E. Merrie, R. J. Marshall and B. R. Parry, *Dis. Colon Rectum*, 2004, **47**, 1341–1349.
2 H. Damon, L. Henry, X. Barth and F. Mion, *Dis. Colon Rectum*, 2002, **45**, 1445–1450.
3 K. D. Hong, J. S. Kim, W. B. Ji and J. W. Um, *Tech. Coloproctol.*, 2017, **21**, 203–210.
4 Y. Maeda, S. Laurberg and C. Norton, *Cochrane Database Syst. Rev.*, 2013, CD007959, DOI: 10.1002/14651858.CD007959.pub3.
5 E. Fournier, C. Passirani, C. N. Montero-Menei and J. P. Benoit, *Biomaterials*, 2003, **24**, 3311–3331.
6 J. M. Anderson, A. Rodriguez and D. T. Chang, *Semin. Immunol.*, 2008, **20**, 86–100.
7 J. B. Schlenoff, *Langmuir*, 2014, **30**, 9625–9636.
8 B. Cao, Q. Tang and G. Cheng, *J. Biomater. Sci., Polym. Ed.*, 2014, **25**, 1502–1513.
9 Y. Takatori, T. Moro, M. Kamogawa, H. Oda, S. Morimoto, T. Umeyama, M. Minami, H. Sugimoto, S. Nakamura, T. Karita, J. Kim, Y. Koyama, H. Ito, H. Kawaguchi and K. Nakamura, *J. Artif. Organs*, 2013, **16**, 170–175.
10 Y. Yamada, S. Saito, T. Nishinaka and K. Yamazaki, *ASAIO J.*, 2012, **58**, 402–406.
11 Z. Cao, L. Zhang and S. Jiang, *Langmuir*, 2012, **28**, 11625–11632.
12 T. F. Carroll, A. Christie, M. Foreman, G. Khatri and P. E. Zimmern, *Int. Braz. J. Urol.*, 2019, **45**, 989–998.
13 C. Sittel, W. F. Thumfart, C. Pototschnig, C. Wittekindt and H. E. Eckel, *J. Biomed. Mater. Res.*, 2000, **53**, 646–650.
14 M. M. Soerensen, L. Lundby, S. Buntzen and S. Laurberg, *Colorectal Dis.*, 2009, **11**, 73–76.
15 L. Brügger, R. Inglin, D. Candinas, T. Sulser and D. Eberli, *Int. J. Colorectal Dis.*, 2014, **29**, 1385–1392.
16 F. Duranti, G. Salti, B. Bovani, M. Calandra and M. L. Rosati, *Dermatol. Surg.*, 1998, **24**, 1317–1325.
17 J. A. Champion, A. Walker and S. Mitragotri, *Pharm. Res.*, 2008, **25**, 1815–1821.
18 P. H. Nijhuis, T. E. Van Den Bogaard, M. J. Daemen and C. G. Baeten, *Dis. Colon Rectum*, 1998, **41**, 624–629.
19 M. Busso and R. Voigts, *Dermatol. Surg.*, 2008, **34**, S16–S24.
20 S. M. Zeitels, P. J. Lombardo, J. L. Chaves, W. C. Faquin, R. E. Hillman, J. T. Heaton and J. B. Kobler, *Ann. Otol., Rhinol., Laryngol.*, 2019, **128**, 71S–81S.
21 S. S. Johl and R. A. Burgett, *Curr. Opin. Ophthalmol.*, 2006, **17**, 471–479.
22 G. Polacco, M. Palla and D. Semino, *Polym. Int.*, 1999, **48**, 392–397.
23 R. Arshady, *Colloid Polym. Sci.*, 1992, **270**, 717–732.
24 C. Kotoulas and C. Kiparissides, *Chem. Eng. Sci.*, 2006, **61**, 332–346.
25 J. Alvarez, J. Alvarez and M. Hernandez, *Chem. Eng. Sci.*, 1994, **49**, 99–113.
26 X. Jin, J. Yuan and J. Shen, *Colloids Surf., B*, 2016, **145**, 275–284.
27 M. Khan, J. Yang, C. Shi, Y. Feng, W. Zhang, K. Gibney and G. N. Tew, *Macromol. Mater. Eng.*, 2015, **300**, 802–809.
28 Y.-H. Gu, H.-W. Liu, X.-H. Dong, Z.-Z. Ma, Y.-X. Li, L. Li, D.-L. Gan, P.-S. Liu and J. Shen, *Rare Met.*, 2022, **41**, 700–712.
29 N. Li, T. Li, X.-Y. Qiao, R. Li, Y. Yao and Y.-K. Gong, *ACS Appl. Mater. Interfaces*, 2020, **12**, 12337–12344.
30 A. Victor, J. Ribeiro and F. S. Araújo, *J. Mech. Eng. Biomech.*, 2019, **4**, 1–9.
31 H. Zhang and M. Chiao, *J. Med. Biol. Eng.*, 2015, **35**, 143–155.

32 A. Gokaltun, M. L. Yarmush, A. Asatekin and O. B. Usta, *Technology*, 2017, **05**, 1–12.
33 V. Cannella, R. Altomare, V. Leonardi, L. Russotto, S. Di Bella, F. Mira and A. Guercio, *BioMed Res. Int.*, 2020, **2020**, 8676343.
34 C. H. Jeong, D. H. Kim, J. H. Yune, H. C. Kwon, D.-M. Shin, H. Sohn, K. H. Lee, B. Choi, E. S. Kim, J. H. Kang, E. K. Kim and S. G. Han, *Toxicol. In Vitro*, 2021, **70**, 105034.
35 K. De Boulle, R. Glogau, T. Kono, M. Nathan, A. Tezel, J.-X. Roca-Martinez, S. Paliwal and D. Stroumpoulis, *Dermatol. Surg.*, 2013, **39**, 1758–1766.
36 M. Zutshi, L. B. Salcedo, P. J. Zaszczurynski, T. L. Hull, R. S. Butler and M. S. Damaser, *Dis. Colon Rectum*, 2009, **52**, 1321–1329.
37 A. Harlim, M. Kanoko and S. Aisah, *Dermatol. Surg.*, 2018, **44**, 1174–1182.
38 K. Ishihara, *J. Biomed. Mater. Res., Part A*, 2019, **107**, 933–943.
39 A. Fallacara, S. Manfredini, E. Durini and S. Vertuani, *Facial Plast. Surg.*, 2017, **33**, 87–96.
40 G. Kaya and F. Oytun, *Biointerface Res. Appl. Chem.*, 2021, **11**, 8424–8430.

